Radiation damage in p-type silicon irradiated with neutrons and protons ☆

Vladimir Cindro [a,*], Gregor Kramberger [a], Manuel Lozano [b], Igor Mandić [a], Marko Mikuž [a], Giulio Pellegrini [b], Jožef Pulko [a], Miguel Ullan [b], Marko Zavrtanik [a]

[a] *Jožef Stefan Institute and University of Ljubljana, Jamova 39, 1000 Ljubljana, Slovenia*
[b] *Centro Nacional de Microelectronica, 0893 Barcelona, Spain*

ARTICLE INFO

ABSTRACT

Diodes fabricated on high resistivity standard, oxygenated and magnetic Czochralski p-type materials were irradiated with reactor neutrons and 24 GeV/c protons up to an equivalent fluence of $\Phi_{eq}=3 \times 10^{14}$ cm^{-2}. Radiation effects on effective trapping times, effective dopant concentration and leakage current were measured at 20 °C. Annealing of defects was performed at 20 and 60 °C.

1. Introduction

The most promising candidates for tracking detectors at the super LHC experiment are silicon detectors fabricated on p-type material [1–3]. Microstrip detectors with n-side readouts have shown acceptable charge collection efficiencies (CCE) after irradiation to high fluences [4]. If the readout electronics are connected to the n-side of a segmented detector, electrons contribute the major part of the signal since they drift towards the higher weighting field. The faster drift of electrons, their lower trapping probability compared to holes and the presence of a high electric field in the region close to the readout electrodes favour n-side readout on the p-type material [5,6]. Bulk damage in silicon causes a change of the effective dopant concentration, an increase of leakage current [7] and trapping of charge carriers [8]. The dominant part of the damage at LHC experiments will be caused by heavy charged particles and neutrons. Their contribution to the radiation field depends on position with respect to the interaction point. Therefore, we measured the degradation of material properties before and after irradiation with protons and neutrons. The first measurements of trapping times in p-type material for particle detectors irradiated with neutrons and protons are presented.

2. Samples and irradiations

Diodes were processed at Centro Nacional de Microelectronica, Barcelona, on three different p-type substrates: high resistivity

($\sim$30 kΩ cm) standard float zone (FZ), diffusion oxygenated float zone (DOFZ) and magnetic Czochralski (MCZ $\sim$3.5 kΩ cm, Okmetics) silicon [9]. The active area of 300 μm thick diodes was 5×5 mm^2. Metallization with a hole on the n-side and mesh on the p-side allowed injection of holes and electrons in the active volume with a laser pulse. The measured concentrations of oxygen in DOFZ and MCZ were $\sim$2 × 10^{17} cm^{-3} and $\sim$5 × 10^{17} cm^{-3}. No data for its concentration in FZ material are available.

Neutron irradiations were performed in the TRIGA nuclear reactor [10] with a flux of 1.9×10^{12} cm^{-2} s^{-1}. Diodes were irradiated to fluences in a range from 0.5×10^{14} cm^{-2} to 3×10^{14} cm^{-2} 1 MeV neutron Non-Ionizing Energy Loss (NIEL) equivalent at 20±1 °C. The neutron flux in the reactor was measured with the leakage current method [11], and the error on the determined fluence was estimated to be ±10%.

Proton irradiations were done at the CERN PS irradiation facility [12] with a 24 GeV/c proton beam with a typical flux of about 10^{10} cm^{-2} s^{-1}. Fluences measured by Al foil activation have ±7% error, while equivalent fluences were calculated with a damage factor of 0.62 [13]. All of the diodes were irradiated at 26±0.5 °C. After irradiation they were kept below 0 °C until the controlled annealing began.

3. Effective doping concentration

Annealing of defects was accelerated by keeping the diodes at 60 °C. Effective doping concentration was calculated from the measured full depletion voltage (V_{FD}). This was determined with the C–V method at 20 °C, 10 kHz frequency and by fitting the $1/C^2$ plot to the measured values. The results are shown in Fig. 1a and b for diodes irradiated by neutrons ($\Phi_{eq}=1 \times 10^{14}$ cm^{-2}) and protons
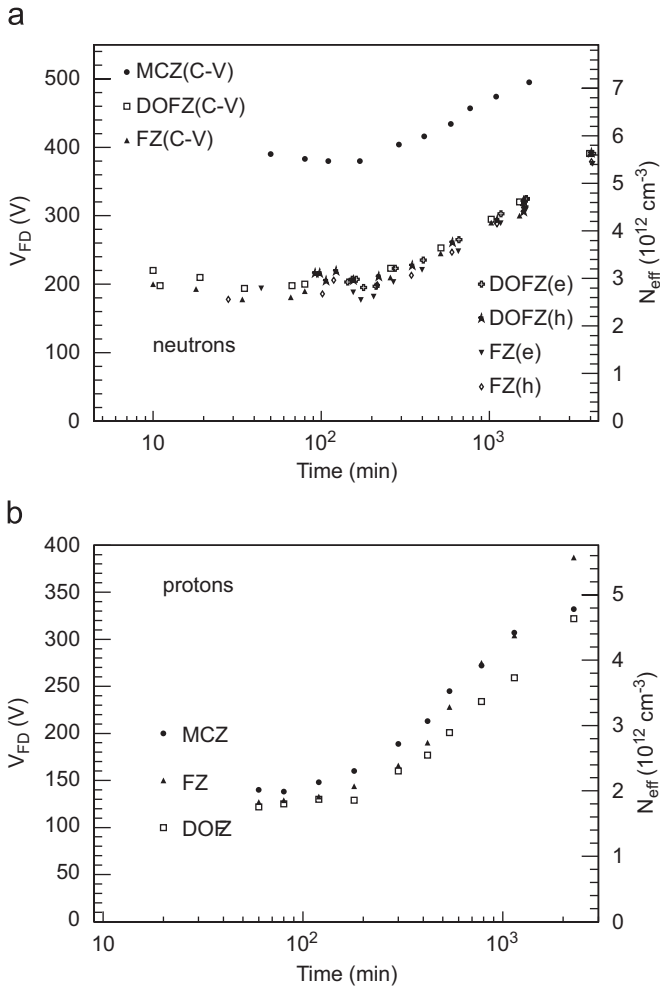
Fig. 1. Time dependence of the full depletion voltage after irradiation with neutrons to $\Phi_{eq}=1 \times 10^{14}\,cm^{-2}$ (a) and protons to $\Phi_{eq}=1.07 \times 10^{14}\,cm^{-2}$ (b). C–V and CCE measurements were taken at 20°. C–V scans were done at 10 kHz frequency, annealing was performed at 60 °C.

Fig. 2. V_{FD} and effective dopant concentration measured after two weeks of annealing at room temperature. Irradiation with neutrons (a) and protons (b).

Table 1
Slope of long-term (reverse) annealing.

	$\Delta N_{eff}/(\Phi_{eq}\Delta t)$ $(10^{-6}\,cm^{-1}\,h^{-1})$		
	$T=20$ °C (protons)	$T=60$ °C (protons)	$T=60$ °C (neutrons)
FZ	3.9 ± 0.4	1510 ± 150	1230 ± 130
DOFZ	2.8 ± 0.3	1380 ± 150	1060 ± 110
MCZ	3.8 ± 0.4	1740 ± 170	1070 ± 110

($\Phi_{eq}=1.07 \times 10^{14}\,cm^{-2}$), respectively. For two sets of diodes (FZ and DOFZ) irradiated with neutrons, the V_{FD} was also determined using measurements of the CCE at 20 °C as the position of a kink in the electron and hole CCE versus voltage plot. All three methods returned a similar time dependence of V_{FD} with a small offset between the measured values (Fig. 1a). In the figures showing the annealing of N_{eff}, we can see three contributions to the space charge: the first with (short) beneficial annealing causing $|N_{eff}|$ to decrease, the second stable over time, and the third with long-term (reverse) annealing. This observation agrees well with the so-called Hamburg model [15], which has been confirmed by irradiations of n-type material. The short-term beneficial annealing that can be clearly seen for neutron-irradiated samples is not evident for proton-irradiated samples. The time constants of short- and long-term annealing are different by several orders of magnitude. Therefore, a stable space charge can be estimated well using measurements of V_{FD} at the minimum in the time dependence plot occurring after 80 min at 60 °C. An extrapolation of the long-term annealing slope to $t=0$ would give more accurate values of the stable space charge; the difference is just a few percent, however, which is negligible compared to the error in the fluence. Measured values of the stable effective dopant concentration obtained from the minima as a function of fluence are shown in Fig. 2a and b for neutrons and protons.
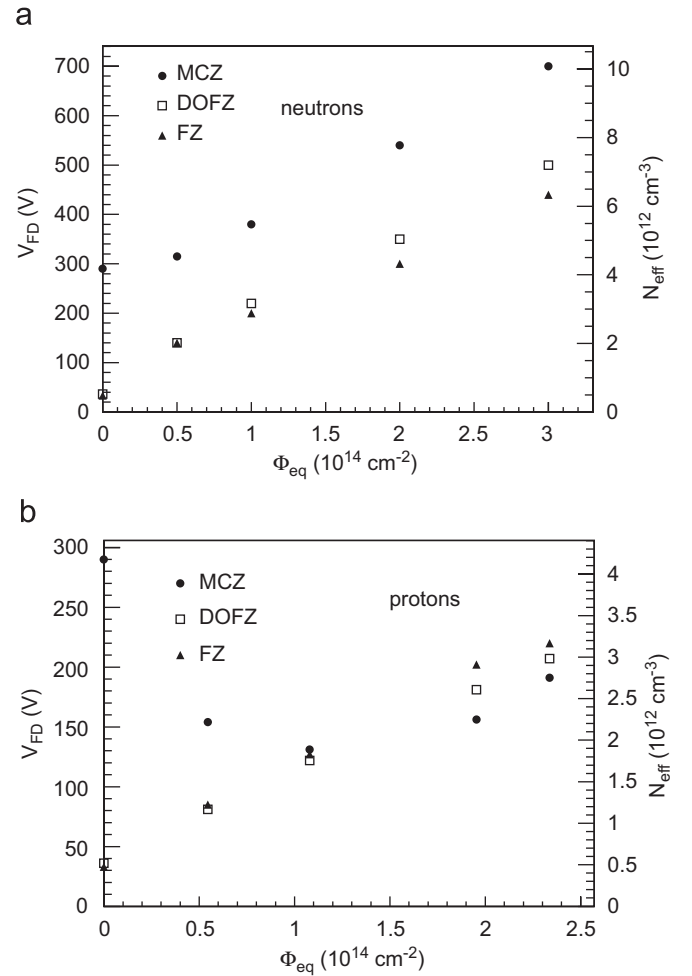
The stable space charge in both the FZ and DOFZ materials is proportional to the fluence. Its change can be parameterized as $\Delta N_{eff}=g_c\Phi_{eq}$, with g_c being a good approximation to the rate of introduction of defects in the Hamburg model [15]. Values of g_c are given in Table 1. On the other hand, the damage in the MCZ material exhibits non-linear behaviour at lower fluences. After irradiation with protons, the $|N_{eff}|$ measured at the minimum in the annealing curve first drops and then starts increasing linearly with fluence (Fig. 2b). The same effect has been observed in previous measurements [16,17] after proton irradiations. There is no space charge sign inversion, which was confirmed by the measurements of TCT signals described in the next section. The drop in $|N_{eff}|$ can be attributed to the mechanism of acceptor removal, while the increase is caused by acceptor creation. Therefore, we calculated the value of g_c for the MCZ material for

a higher proton fluence range ($>10^{14}\,\mathrm{cm}^{-2}$), where most of the acceptor removal has been completed. This value of g_c is about 50% higher than previous measurements [16,17]. While proton irradiation removed all the initially existing acceptors in the MCZ material for fluences above $\Phi_{\mathrm{eq}}=2\times10^{14}\,\mathrm{cm}^{-2}$, acceptor removal is less evident for neutron irradiation where only a small part of initially present effective acceptors was removed (Fig. 2a). Stable damage caused by neutron irradiation agrees well with the measurements for n-type materials [18,19].

One set of diodes irradiated with protons to $\Phi_{\mathrm{eq}}=1.95\times10^{14}$ cm^{-2} was annealed at 20 °C, and the results of V_{FD} measurements are shown in Fig. 3. The effective dopant concentration N_{eff} was determined from V_{FD}, and the slope $\Delta N_{\mathrm{eff}}/(\Phi_{\mathrm{eq}}\Delta t)$ was calculated using a linear fit in the first stage of reverse annealing. The linear function was fitted to measured points in the 400–1400 h interval at 20 °C and the 200–600 min interval at 60 °C. In these intervals, the linear fit agrees well with the measured data since short-term annealing is already completed and the long-term (reverse) annealing time constants are long compared to the interval width. Statistical errors of fit and error due to temperature inaccuracy (±0.5 °C) are much smaller than the errors in the fluence, and therefore the error of the slope is dominated by the latter. The determined values of the slopes are given in Table 2.

The measured values of the slopes for all three p-type materials are comparable at the same temperature. For proton-irradiated samples, the acceleration factor of reverse annealing calculated from the ratio of slopes measured at 60 and 20 °C is 440 ± 40. Using the Arrhenius relation [14] for the temperature dependence of reverse annealing and assuming that the introduction rate of the reverse annealing component is independent of the fluence, we obtain $E_a=1.28\pm0.03$ eV. This value agrees with the value of $E_a=1.31\pm0.04$ eV measured for reverse annealing of irradiated n-type silicon [15].

The leakage current measured in the three different materials was equal within a few percent for all the samples irradiated to the same fluence.
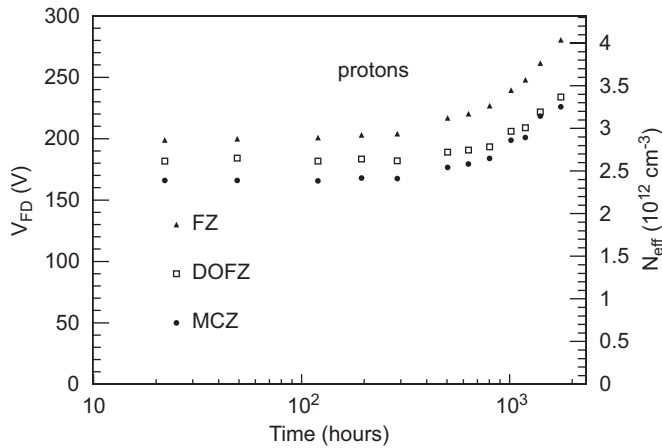
4. Trapping time parameter

Trapping times were measured at 20 °C with the charge correction method [20,21]. This method is based on the measurements of signals induced in pad detectors by drifting electrons or holes. A detailed explanation of the experimental setup can be found in Refs. [6,20]. The highest voltage that could be applied was limited by breakdown in the diodes and was between 450 and 900 V, depending on the sample.

The effective trapping probability $1/\tau_{\mathrm{e,h}}$ for electrons and holes at a given temperature T and time t after irradiation was parameterized as Ref. [20]:

$$\frac{1}{\tau_{\mathrm{e,h}}} = \beta_{\mathrm{e,h}}(T,t)\times\Phi_{\mathrm{eq}}. \tag{1}$$

The trapping time parameter $\beta_{\mathrm{e,h}}$ measures the effect of irradiation on trapping. It was determined by fitting a linear function to the measured effective trapping probabilities after neutron irradiation to different fluences (Fig. 4a and b). The samples were annealed for 80 min at 60 °C before the measurements were performed. The values extracted from the fit are presented in Table 3. We may notice that the linear fit returns overly low values of β at lower fluence values and overly high values at higher fluences when compared to the measured values. A similar

Fig. 3. Annealing of full depletion voltage measured with C–V method at 20° after irradiation with protons to $\Phi_{\mathrm{eq}}=1.95\times10^{14}\,\mathrm{cm}^{-2}$.

Table 2
Parameter g_c measuring the stable damage.

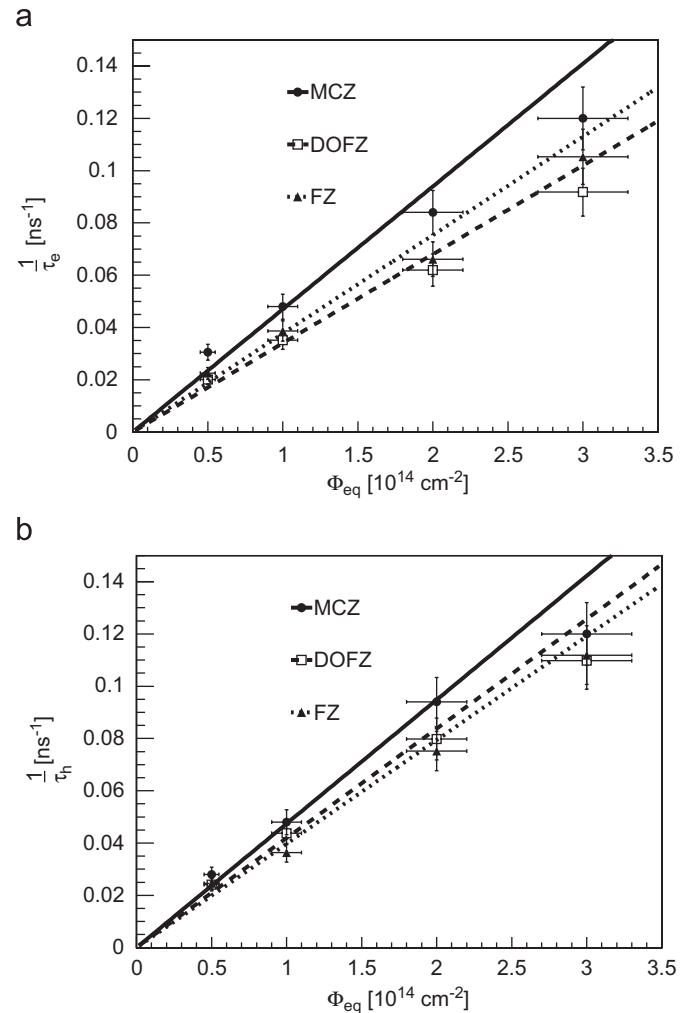|	FZ (cm^{-1})	DOFZ (cm^{-1})	MCZ (cm^{-1})
Neutrons	0.017 ± 0.002	0.020 ± 0.002	0.022 ± 0.002
Protons	0.012 ± 0.001	0.010 ± 0.001	0.013 ± 0.001

Fig. 4. Fluence dependence of the effective trapping probability after neutron irradiation for electrons (a) and holes (b). Measurements were taken at $T=20$ °C. A linear fit to the measured values is shown. FZ—dotted line, DOFZ—dashed line, MCZ—solid line.

Table 3

Trapping parameter β measured after neutron irradiation in three different p-type materials.

	FZ	DOFZ	MCZ
β_e (10^{-16} cm^{-2} ns^{-1})	3.8 ± 0.4	3.4 ± 0.3	4.7 ± 0.4
β_h (10^{-16} cm^{-2} ns^{-1})	4.0 ± 0.4	4.2 ± 0.4	4.7 ± 0.4

β_e stands for electrons and β_h for holes. The equivalent neutron fluences used in the fit ranges from 0.5×10^{14} cm^{-2} to 3.0×10^{14} cm^{-2}.

conclusion, although not so evident, could be drawn from some of the measurements in Ref. [6]. This indicates that a linear extrapolation to higher fluences may not be correct and that measurements of trapping times at higher fluences are needed. The previously measured values for n-type material at the same temperature are $\beta_e=(4.0\pm0.4)\times10^{-16}$ cm^2 ns^{-1} and $\beta_h=(5.4\pm0.6)\times10^{-16}$ cm^2 ns^{-1} [6]. Electron trapping measured in p-type material after 80 min of annealing at 60 °C agrees well with that measured in n-type material. The hole trapping measured in p-type material is slightly lower than that measured in n-type material; however, errors in the measurements do not allow a final conclusion. The same is valid for the higher trapping observed in p-type MCZ material. All these differences are small, and more measurements are needed to get a clearer picture.

4.1. Trapping time parameter during annealing

It has been observed that trapping times measured in n-type material change after annealing at elevated temperatures [6,22,23], with trapping times of electrons increasing by about 35% and hole trapping times decreasing by about 30%. On the other hand, measurements of CCE with a minimum ionizing particle in silicon microstrip detectors fabricated on p-type material using n-strip readouts have shown practically no change after annealing [24]. Therefore, we performed the measurements of trapping on p-type material after annealing at 60 °C. The annealing was done for diodes irradiated to the equivalent fluence $\Phi_{eq}=10^{14}$ cm^{-2} with neutrons and $\Phi_{eq}=1.07\times10^{14}$ cm^{-2} with protons. The trapping parameter β was calculated from Eq. (1), and the results are shown in Fig. 5a and b for neutron and proton-irradiated diodes, respectively. All measurements of trapping times were done at 20 °C. The experimental errors on the measured trapping parameter β are about 10% without taking into account the error of the fluence. This error was estimated by changing the size and position of the interval of the voltages in which the charge correction method was applied. The longest annealing time was limited by breakdowns that happened in the later stage of annealing due to increasing V_{FD}. In such cases the interval used in the charge correction method became too small for a reliable determination of the trapping time. Diodes with higher breakdown voltages would improve the accuracy of the measurements and allow longer annealing times.

An exponential function of the form [22]

$$\beta_{e,h} = \beta_{0,e,h} e^{-t/\tau_{ann,e,h}} + \beta_{\infty,e,h}(1 - e^{-t/\tau_{ann,e,h}}) \quad (2)$$

was fitted to the measured values of the trapping parameter $\beta_{e,h}$. The values extracted from the fit and their errors are gathered in Table 4. In some cases, the fit did not converge to meaningful results, and the parameters of the exponential function are not given in the table. Nevertheless, we may conclude that in the annealing process, the trapping of holes undergoes more change than the trapping of electrons. This is more evident in the FZ and DOFZ material than in the MCZ material. After several thousands of minutes of annealing, β_h is about two times higher than β_e for
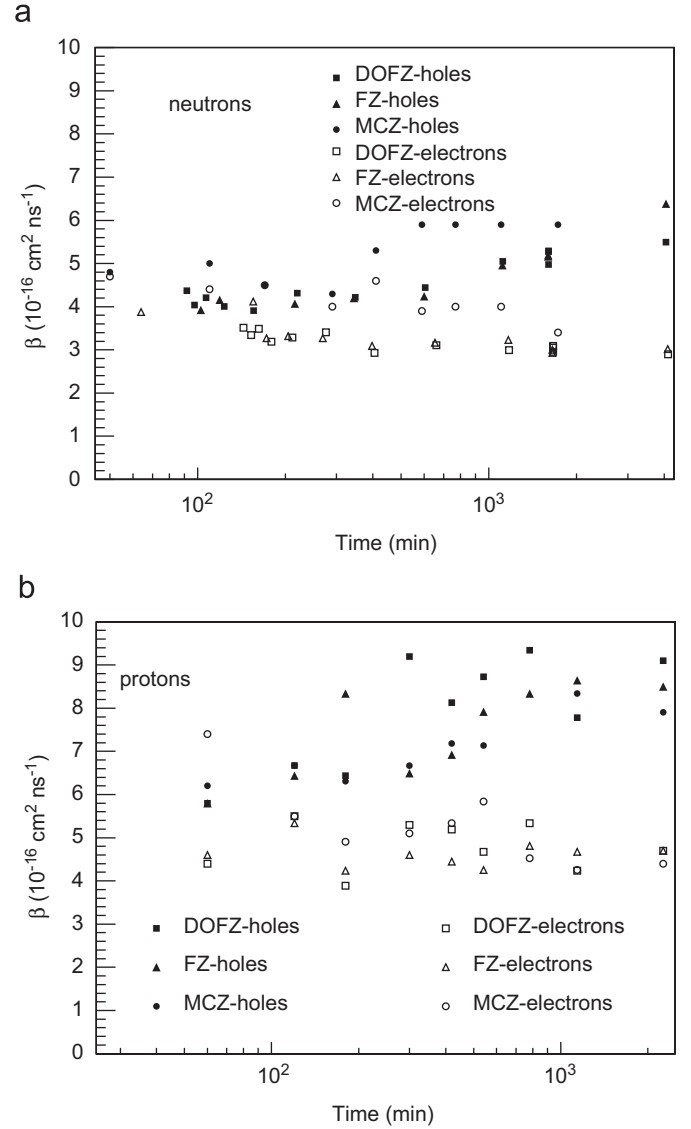
Fig. 5. Trapping parameter β measured at $T=20$ °C after annealing at 60 °C for diodes irradiated with neutrons to $\Phi_{eq}=10^{14}$ cm^{-2} (a) and protons to $\Phi_{eq}=1.07\times10^{14}$ cm^{-2} (b).

both neutron and proton irradiation. It can also be seen that protons are more damaging than neutrons in terms of trapping at the same NIEL. The difference is about 40% after annealing. These conclusions are in agreement with measurements of n-type material; however, the accuracy of the measurements is not good enough for a more detailed comparison of the numerical values obtained from the fit in p and n-type material.
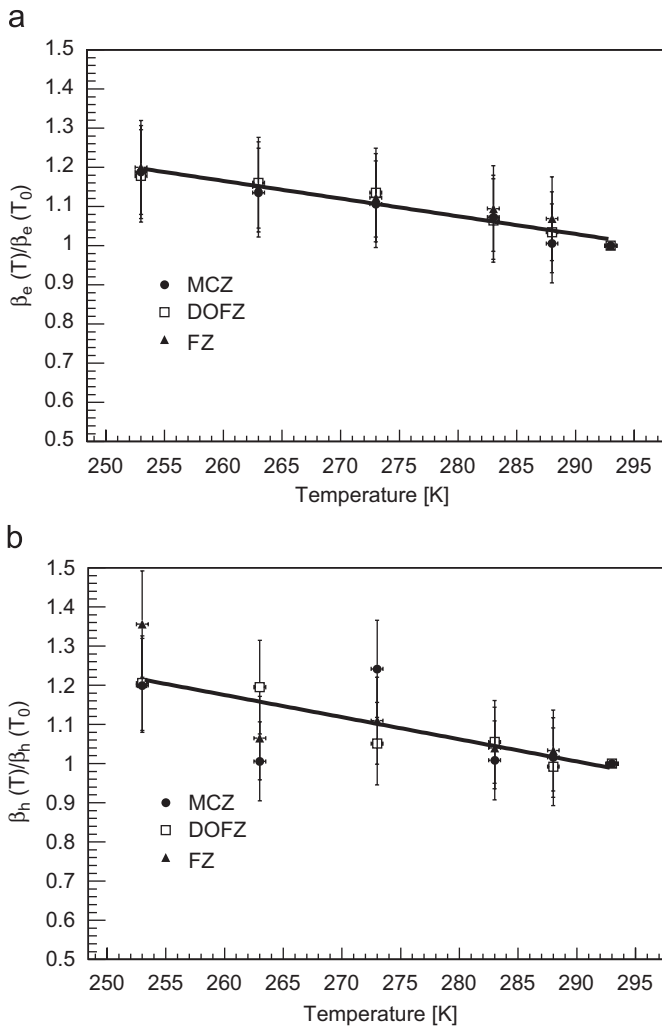
4.2. Temperature dependence of the trapping parameter

Trapping times depend on the temperature that affects the thermal velocity, trap occupancy and cross sections for trapping [6]. We measured trapping times in the temperature range between −20 and 20 °C, covering the range of cooled large scale experiments and laboratory room temperature measurements. The relative values of the trapping parameter β are plotted in Fig. 6 for diodes irradiated with neutrons to $\Phi_{eq}=5\times10^{12}$ cm^{-2}. Diodes were annealed for 80 min at 60 °C before the measurements took place, and the measurements are normalized to the value measured at $T=20$ °C. Higher values of trapping were measured at

Table 4
Parameters extracted from the fit of two exponential functions (Eq. (2)) to the measured values of the trapping parameter during annealing at 60 °C.

		Neutrons			Protons		
		β_0	τ_{ann} (min)	β_∞	β_0	τ_{ann} (min)	β_∞
Holes	DOFZ	3.9±0.1	1320+620−400	5.6+0.3−0.2	4.5+1.0−1.3	180+130−170	8.7±0.5
	FZ	3.8±0.1	3180+2100−970	7.4+1.4−1.7	5.8+0.6−0.8	500+700−270	8.7±0.8
	MCZ	4.4±0.4	840+1100−500	6.3±1.0	6.0±0.3	600+450−220	8.2±0.3
Electrons	DOFZ	4.1+1.5−0.5	157+160−75	3.0±0.1	4.3±0.9		
	FZ	4.4±0.5	155+100−50	3.0±0.1	4.5±0.5		
	MCZ	4.5±0.2			6.4+1.0−0.7	400+1000−200	4.3±0.5

Trapping parameters are expressed in units of $(10^{-16}\,\mathrm{cm}^{-2}\,\mathrm{ns}^{-1})$.

Fig. 6. Temperature dependence of electron (a) and hole (b) trapping probability. Measurements are normalized to the value measured at T=293 K.

lower temperatures. In the temperature domain, a linear fit gives good agreement with the data and was used instead of the more sophisticated fit used in Ref. [6]. The measured slope of $\beta(T)/\beta(20°)$ is $-0.004\,\mathrm{K}^{-1}$ for electrons and $-0.006\,\mathrm{K}^{-1}$ for holes. These values are in good agreement with those given by a linear fit to the data measured in n-type materials, which are -0.003 and $-0.006\,\mathrm{K}^{-1}$ [6].

5. Conclusions

Measurements of N_{eff} after irradiation with neutrons and protons at fluences of several times $10^{12}\,\mathrm{cm}^{-2}$ showed that effectively stable acceptors are created in all three types of measured p-type materials. The stable damage creation rate with neutrons ($\approx 0.02\,\mathrm{cm}^{-1}$) is comparable to the damage creation rate measured for n-type material. The acceptor removal is the most evident after proton irradiation in the MCZ material, where most of the initially present acceptors were removed. The stable damage creation rate at higher proton fluences ($\approx 0.01\,\mathrm{cm}^{-1}$) is approximately two times lower than that with neutrons, and it did not show any difference between the three materials indicating that high concentrations of oxygen could be present in the standard FZ material. The measured activation energy of reverse annealing is E_a=1.28±0.03 eV. The leakage current did not depend on the material type and agrees with previously measured values within experimental error.

Measurements of trapping times at 20 °C and after annealing at 60 °C in p-type standard and DOFZ Si as well as in MCZ Si have shown no significant difference when compared to values measured in n-type material. Values of trapping damage constants slightly decrease with fluence, however in the measured fluence range their average value agrees well with previous results in n-type silicon.

Acknowledgements

References

[1] A. Seiden, LHC Upgrade R&D, in: Presented at Second Trento Workshop on Advanced Silicon Detectors (3D and p-type), Trento, February 13–14, 2006.
[2] E. Fretwurst, et al., Nucl. Instr. and Meth. A 552 (2005) 7.
[3] H. Sadrozinski, Nucl. Instr. and Meth. A 552 (2005) 1.
[4] G. Casse, P.P. Allport, S. Martí i Garcia, M. Lozano, P.R. Turner, Nucl. Instr. and Meth. A 535 (2004) 362.
[5] G. Kramberger, V. Cindro, I. Mandić, M. Mikuž, M. Zavrtanik, IEEE Trans. Nucl. Sci. NS-49 (4) (2002) 1717.
[6] G. Kramberger, V. Cindro, I. Mandić, M. Mikuž, M. Zavrtanik, Nucl. Instr. and Meth. A 481 (2002) 297.
[7] G. Lindström, et al., Nucl. Instr. and Meth. A 466 (2001) 308.
[8] H.W. Kraner, Z. Li, E. Fretwurst, Nucl. Instr. and Meth. A 326 (2003) 350.
[9] G. Pellegrini, et al., Nucl. Instr. and Meth. A 548 (2005) 355.
[10] M. Ravnik, R. Jeraj, Nucl. Sci. Eng. 145 (1) (2003) 145.
[11] M. Moll, E. Fretwurst, G. Lindstrom, Nucl. Instr. and Meth. A 426 (1999) 87.
[12] M. Glaser, F. Ravotti, IEEE Trans. Nucl. Sci. NS-53 (4) (2006) 2016.

[13] M. Moll, E. Fretwurst, M. Kuhnke, G. Lindström, Nucl. Instr. and Meth. B 186 (2002) 100.

[14] S. Arrhenius, Z. Physik. Chem. 4 (1889) 226.

[15] G. Lindström, M. Moll, E. Fretwurst, Nucl. Instr. and Meth. A 426 (1999) 1.

[16] M. Bruzzi, et al., Nucl. Instr. and Meth. A 552 (2005) 20.

[17] H. Hoedelmoser, M. Moll, M. Koehler, H. Nordlund, Nucl. Instr. and Meth. A 583 (2007) 64.

[18] D. Žontar, et al., Nucl. Instr. and Meth. A 426 (1999) 51.

[19] M. Moll, E. Fretwurst, G. Lindstroem, Nucl. Instr. and Meth. A 439 (2000) 282.

[20] G. Kramberger, V. Cindro, I. Mandić, M. Mikuž, M. Zavrtanik, Nucl. Instr. and Meth. A 476 (2002) 645.

[21] T.J. Brodbeck, A. Chilingarov, T. Sloan, E. Fretwurst, M. Kuhnke, G. Lindstroem, Nucl. Instr. and Meth. A 455 (2000) 645.

[22] G. Kramberger, M. Batič, V. Cindro, I. Mandić, M. Mikuž, M. Zavrtanik, Nucl. Instr. and Meth. A 571 (2007) 608.

[23] O. Krasel, C. Gossling, R. Klingenberg, S. Rajek, R. Wunstorf, IEEE Trans. Nucl. Sci. NS-51 (2004) 3055.

[24] G. Casse, P.P. Allport, A. Watson, Nucl. Instr. and Meth. A 568 (2006) 46.